Modulation of N^N'-bidentate chelating pyridyl-pyridylidene amide ligands offers mechanistic insights into Pd-catalysed ethylene/methyl acrylate copolymerisation

Gearóid M. Ó Máille,[a] Anna Dall'Anese,[b,c] Philipp Grossenbacher,[a] Tiziano Montini,[b] Barbara Milani,[b,]* and Martin Albrecht[a,]*

[a]Department of Chemistry & Biochemistry, University of Bern, Freiestrasse 3, CH-3012 Bern, Switzerland

[b]Dipartimento di Scienze Chimiche e Farmaceutiche, Università di Trieste, Via Licio Giorgieri 1, 34127 Trieste, Italy

[c]Current address: Department of Chemistry, Biology and Biotechnology, University of Perugia, Via Elce di Sotto 8, 06123 - Perugia, Italy

E-mail: milaniba@units.it; martin.albrecht@dcb.unibe.ch

ORCID:

Gearóid M. Ó Máille:	0000-0001-9793-0973
Anna Dall'Anese:	0000-0001-6286-489X
Philipp Grossenbacher:	0000-0001-8266-6882
Tiziano Montini:	0000-0001-9515-566X
Barbara Milani:	0000-0002-4466-7566
Martin Albrecht:	0000-0001-7403-2329

Abstract

The efficient copolymerisation of functionalised olefins with alkenes continues to offer considerable challenges to catalyst design. Based on recent work using palladium complexes containing a dissymmetric N^N'-bidentate pyridyl-PYA ligand (PYA = pyridylidene amide), which showed a high propensity to insert methyl acrylate, we have here modified this catalyst structure by inserting shielding groups either into the pyridyl fragment, or the PYA unit, or both to avoid fast β-hydrogen elimination. While a phenyl substituent at the pyridyl side impedes catalytic activity completely and leads to an off-cycle cyclometallation, the introduction of an ortho-methyl group on the PYA side of the N^N'-ligand was more prolific and doubled the catalytic productivity. Mechanistic investigations with this ligand system indicated the stabilisation of a 4-membered metallacycle intermediate at room temperature,

1

which has previously been postulated and detected only at 173 K, but never observed at ambient temperature so far. This intermediate was characterised by solution NMR spectroscopy and rationalises, in part, the formation of α,β-unsaturated esters under catalytic conditions, thus providing useful principles for optimised catalyst design.

Introduction

Advances in modern technology have led to an unprecedented demand for materials which display tunable and controllable properties. This has prompted a drive to modify commodity plastics, such as polyethylene, in order to satisfy these requirements. In particular, it is expected that the incorporation of polar vinyl monomers into the polyethylene backbone imparts superior surface properties, such as adhesion, dyeability and printability, to mention a few, onto the polymer, although this has presented its own challenges.[1,2,3,4,5,6,7] Indeed, traditional catalysts for the industrial synthesis of polyolefins, based on early transition metals (such as the Ziegler Natta-type catalysts), are very oxophilic and, therefore, incompatible with such polar functional groups. Radical polymerisation suffers from expensive high-pressure requirements, alongside a lack of controllability, which is also a severe setback encountered in post-polymerisation modification. A significant step forward was achieved by Brookhart and co-workers, who demonstrated that Ni(II) and Pd(II) complexes bearing sterically hindered α-diimines show high catalytic activity in ethylene homopolymerisation leading to high molecular weight polyethylene thanks to their capability of sterically blocking ligand substitution and, thus, preventing chain transfer.[8,9]

Alongside the benefits of providing a degree of control over polymer microstructure and molecular weight distribution, these late transition metal systems are far less oxophilic, opening the door to controlled polar vinyl monomer incorporation in olefin-derived polymers.[10,11] Pd(II) and Ni(II) complexes bearing N^N ligands derived from Brookhart's motif based on an acenaphthene (Ar-BIAN) or 1,4-diaza-1,3-butadiene skeleton (Ar-DAB, see Fig. 1) have dominated this field for decades, as they display a reasonable polar monomer tolerance and, generally, good productivity of highly branched copolymers with the polar groups decorating the end of the branches.[12,13,14] Early work by Drent, Pugh *et al.*[15] showed the benefit of using unsymmetrical P-O donor ligands (Fig. 1): these give excellent compatibility with a wide array of polar monomers and yield linear macromolecules with a high degree of polar monomer incorporation in the main chain.[16] The low productivity together with too high an incorporation

of the polar monomer, however, hamper large scale exploitation.[17] Other Pd and Ni complexes based on hybrid ancillary ligands have also been investigated recently (Fig. 1).[18]
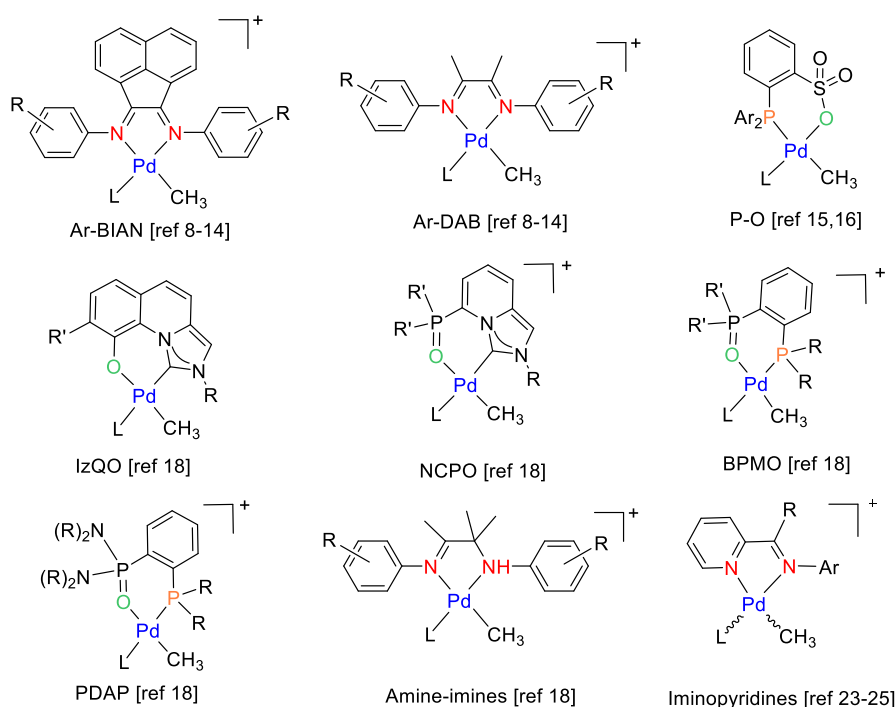

Fig. 1 A selection of complexes used in Pd-catalysed ethylene/acrylic esters copolymerisation (L = neutral solvent ligand).

The concept of "unsymmetrical" ligands, introduced with the P-O donor system, has been extrapolated to the archetypal N^N coordinating α-diimines by one of us in order to introduce a bias in the donor strength of the coordinating nucleus.[19,20] This strategy yields precatalysts which have a significantly higher productivity of co-oligomers than their symmetrical analogues. Ethylene/methyl acrylate (MA) copolymers were produced with unsymmetrical α-diimines sharing benzhydryl groups on one of the two aryl rings.[21,22] Another class of versatile unsymmetrical ligands is constituted by iminopyridines, which have found successful application in Pd-catalysed CO/vinyl arene copolymerisation.[23,24,25] As an extension of this approach, we have recently demonstrated that Pd(II) complexes bearing bidentate pyridylidenamide (PYA)-derived ligands rapidly catalyse the dimerisation of ethylene and give a high degree of methyl acrylate (MA) incorporation, though rapid chain transfer yielded only low molecular weight products.[26]
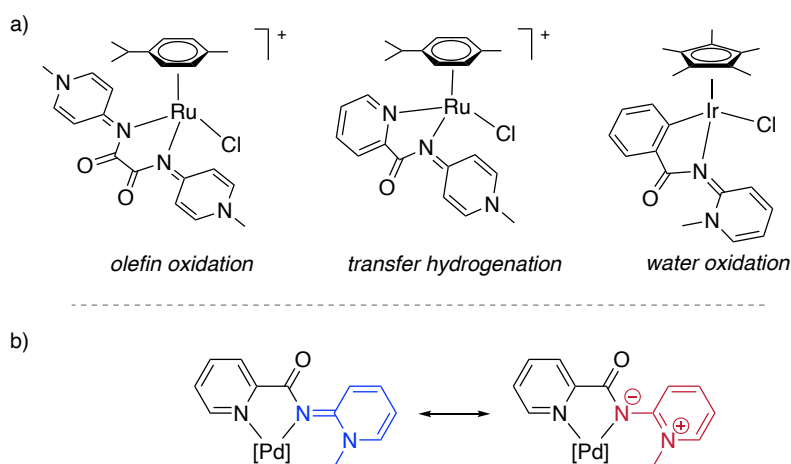
Scheme 1 a) Recent examples of catalytically active PYA complexes with *para-* and *ortho-* pyridylidene components; b) pyridyl-PYA scaffold at palladium with relevant resonance structures of the *ortho-*PYA ligand.

These PYA ligands have great potential for tailored catalysis since they are readily functionalisable and electronically flexible due to their ability to exist in configurations with varying contributions from zwitterionic and neutral forms (Scheme 1).[27,28,29,30] In order to take advantage of the Pd-PYA system in the production of higher molecular weight co-polymers, however, the observed rapid chain transfer must be suppressed. We postulate that increasing steric hindrance around the metal centre will have a dual effect, firstly in slowing the rate of β-hydride elimination, and secondly in optimising the rate of monomer coordination to control the formation of co-polymers. With an appropriate balance of steric hindrance, the strong bias between the two distinct N-donor sites of the pyridyl-PYA ligand offers potential to promote efficient olefin insertion, while the PYA donor flexibility may induce mobility in the metal-bound species *via* the *trans* effect. Here we provide support for this hypothesis and further demonstrate that the electronic flexibility of this PYA system leads to the stabilisation of a rarely detectable 4-membered palladacycle intermediate, which leads to a unique product profile.

Results and Discussion

The readily adaptable synthesis of the PYA ligand facilitates straightforward modification of the complex's periphery. In this work, a series of complexes were synthesised in which the steric bulk around the N-donor sites of the N^N' bidentate ligand is increased in a systematic manner when compared to the parent pyridyl-PYA complex **9** reported previously by us (Scheme 2).[26] Specifically, attempts to limit rotation of the PYA unit involved the introduction

of a methyl group in the PYA 3-position (complex **10**), while a phenyl substituent on the pyridyl 6-position was assumed to shield the pyridyl side of the complex (complex **11**). Complex **12** contains both of these substituents to combine either effect.
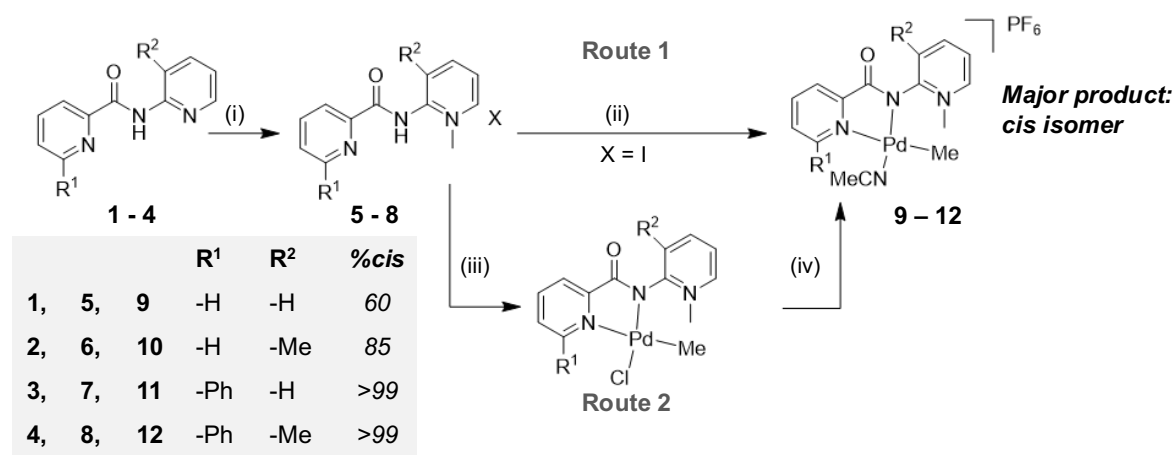
Scheme 2 Synthesis of the ligands **5–8**; (i) MeI, CH$_2$Cl$_2$; synthesis of Pd complexes **9–12**: Route 1:(ii) [Pd(COD)(Me)Cl], K$_2$CO$_3$ and AgPF$_6$ in MeCN; Route 2: (iii) first NH$_4$PF$_6$ in MeCN, then [Pd(COD)(Me)Cl], K$_2$CO$_3$ in CH$_2$Cl$_2$, (iv) NH$_4$PF$_6$ in MeCN.

Synthesis

The new ligand precursors **6–8** were synthesised in a manner analogous to that previously reported for **5** by reacting the appropriate acid chloride with commercially available 2-amino-pyridines to yield amides **1–4**, which were subsequently methylated using MeI (Scheme 2). Two strategies were employed in order to form the [Pd(Me)(MeCN)(PYA)][PF$_6$] complexes **9–12**. Route 1 followed the one-pot method established earlier,[26] consisting of reacting [Pd(COD)(Me)Cl], K$_2$CO$_3$ and AgPF$_6$ with the iodo salt of the proligand in MeCN. The new alternative route, route 2, was devised in order to eliminate traces of silver that might potentially interfere in catalytic conversion. This method involves exchanging the anion in the ligand precursor from iodide to PF$_6^-$, followed by metalation with the Pd precursor in the presence of K$_2$CO$_3$ to yield the chlorido complexes [Pd(PYA)(Me)Cl]. Stirring these complexes in MeCN in the presence of an excess of NH$_4$PF$_6$ furnished the solvento complexes with identical analytical data as those obtained from route 1. Since the N^N bidentate pyridyl-PYA ligand is nonsymmetric, the Pd-bound methyl group can assume two distinct positions,

viz. either *cis* or *trans* to the PYA nitrogen atom. In the ^{1}H NMR spectrum of complex **9**, both isomers are detectable by the two characteristic Pd-Me signals in a 3:2 ratio, with the signal of the *cis* isomer shielded relative to that of the *trans* isomer due to ring-current effects from the nearby PYA ring ($\delta_{H\ cis}$ = 0.10 ppm, $\delta_{H\ trans}$ = 1.01 ppm). The same pattern is observed with complex **10**, with the ^{1}H NMR signals for the *cis* (δ_H = –0.05 ppm) and *trans* Pd-Me (δ_H = 0.98 ppm) resonance integrations indicating a 6:1 isomer ratio, again favouring the *cis* form. The higher *cis/trans* ratio observed for **10** with respect to **9** might be ascribed to the presence of the methyl group on the PYA ring, which enhances the difference in donor capability between N_{pyr} and N_{PYA} towards the latter, thus favoring coordination of the methyl to palladium preferentially *cis* to the more donating N_{PYA} site. ^{1}H NMR spectra of complexes **11** and **12** show only a single Pd–Me resonance (δ_H = 0.06 ppm and –0.07 ppm respectively), indicating the presence of the *cis* isomer exclusively. Presumably, the increased steric bulk of the pyridyl-bound phenyl group precludes the formation of the *trans* isomer. Assuming an unaltered ring current effect, the Pd–Me singlet of the *cis* isomer can be used as a probe for the electron density on the palladium centre, and hence as a proxy for the donor capability of the PYA ligand.[24, 28] Accordingly, the similar and strongly shielded Pd–Me shifts of complexes **10** and **12** (δ_H = –0.05 and –0.07 ppm, respectively), both bearing an electron donating R^2 methyl group, indicate an increased donor strength of the appended PYA ligand fragment compared to complexes **9** and **11** (δ_H = +0.10 and +0.06 ppm, respectively).

Oligomerisation catalysis

Each complex was screened for catalytic activity in ethylene/MA co-oligomerisation. Standard conditions for these experiments were a [MA]/[Pd] ratio of 600, reaction time of 18 h at 308 K under 2.5 bar ethylene. 2,2,2-Trifluoroethanol (TFE) was used as solvent due to its ability to stabilise Pd-hydride species.[31] The products of the catalytic runs were analysed by GC-MS of the reaction mixture and subsequent NMR spectroscopy of the vacuum-dried residue. Under these conditions, **9** gave the same product profile as previously reported, namely a mixture of 2-butenes and pentenoates,[26] and provided a useful reference point. A run with a sample of **9** synthesised *via* the silver-free route 2 gave the same products according to NMR and GC-MS analyses, and the same modest productivity based on the weight of recovered non-volatile material (Table 1, Scheme 3). The identical performance of these different batches of **9** indicates that the synthetic route involving silver salts is unproblematic. Complexes **11** and **12** bearing a sterically congested pyridyl group, were essentially inactive. When using complex **12** as the most hindered complex in the series, significant palladium mirror was observed

within 2 h and only free ligand was recovered following the catalytic run. The latter results are remarkably different with respect to those obtained with Ni(II) catalysts having 6-substituted pyridylimino ligands, which lead to low molecular weight ethylene/MA copolymers.[32]
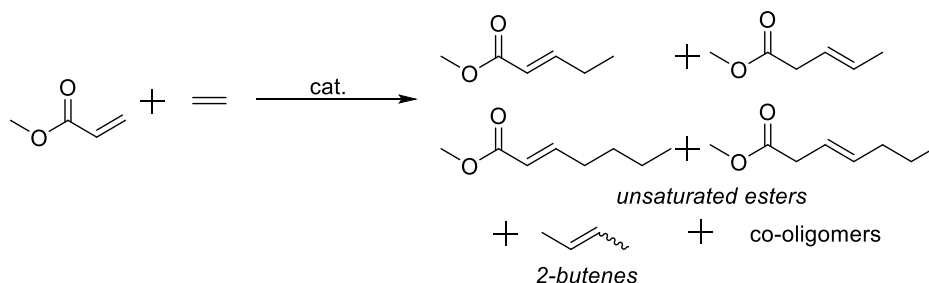
Scheme 3 Ethylene/MA co-oligomerisazation; cat: complexes **9–12**.

Table 1. Ethylene/MA co-oligomerisations with complexes **9–12**[a].

Precat	Yield	Productivity[b]	Products[c]:	
	(mg)	(g P/g Pd)	NMR	GC-MS
9	22.6	10.4	α,β- and β,γ-unsaturated esters	butenes, hexenes, pentenoic and heptenoic esters (traces)
9[d]	20.6	9.5	α,β- and β,γ-unsaturated esters	butenes, hexenes, pentenoic and heptenoic esters (traces)
10	58.5	26.6	α,β- and β,γ-unsaturated esters, co-oligomeric species	pentenoic (traces) and heptenoic esters
11		-	decomposition products	no significant signals
11[d]		-	decomposition products	no significant signals
12		-	small amount of free ligand	no significant signals

[a] Reaction conditions: n_{Pd} = 21 μmol, TFE V = 21 mL, [MA]/[Pd] = 600, $P_{ethylene}$ = 2.5 bar, T = 308 K, t = 18 h; [b] g P/g Pd = grams of product per gram of palladium; [c] as determined by NMR or GC-MS; [d] catalyst prepared via silver-free route 2, *cf* Scheme 2.

Complex **10**, however, gave more promising results and revealed activity of the palladium centre in this complex. Figure 2 compares the ^{1}H NMR spectra of the recovered non-volatiles from catalytic runs using complexes **9** and **10** and an example of a typical MA/ethylene co-

oligomer obtained under identical conditions using an analogous catalyst with a nonsymmetric Ar-DAB ligand.[20] NMR analysis revealed that complex **9** gives predominantly *trans α,β*-unsaturated esters, as indicated by the characteristic alkene doublets of triplets at $\delta_H = 6.96$ and 5.83 for the *β* and *α* CH, respectively, together with *trans β,γ*-unsaturated esters characterised by the multiplet at 5.52 ppm for the *β* and *γ* CH and the diagnostic *α* CH$_2$ doublet at 3.00 ppm (Fig. 2). Complementary GC-MS studies confirmed the formation of pentenoic and heptenoic esters. Catalytic runs with **10** produced the same ester species, though additionally, significant amounts of co-oligomeric products were also observed (Figures 2, S15, S16).
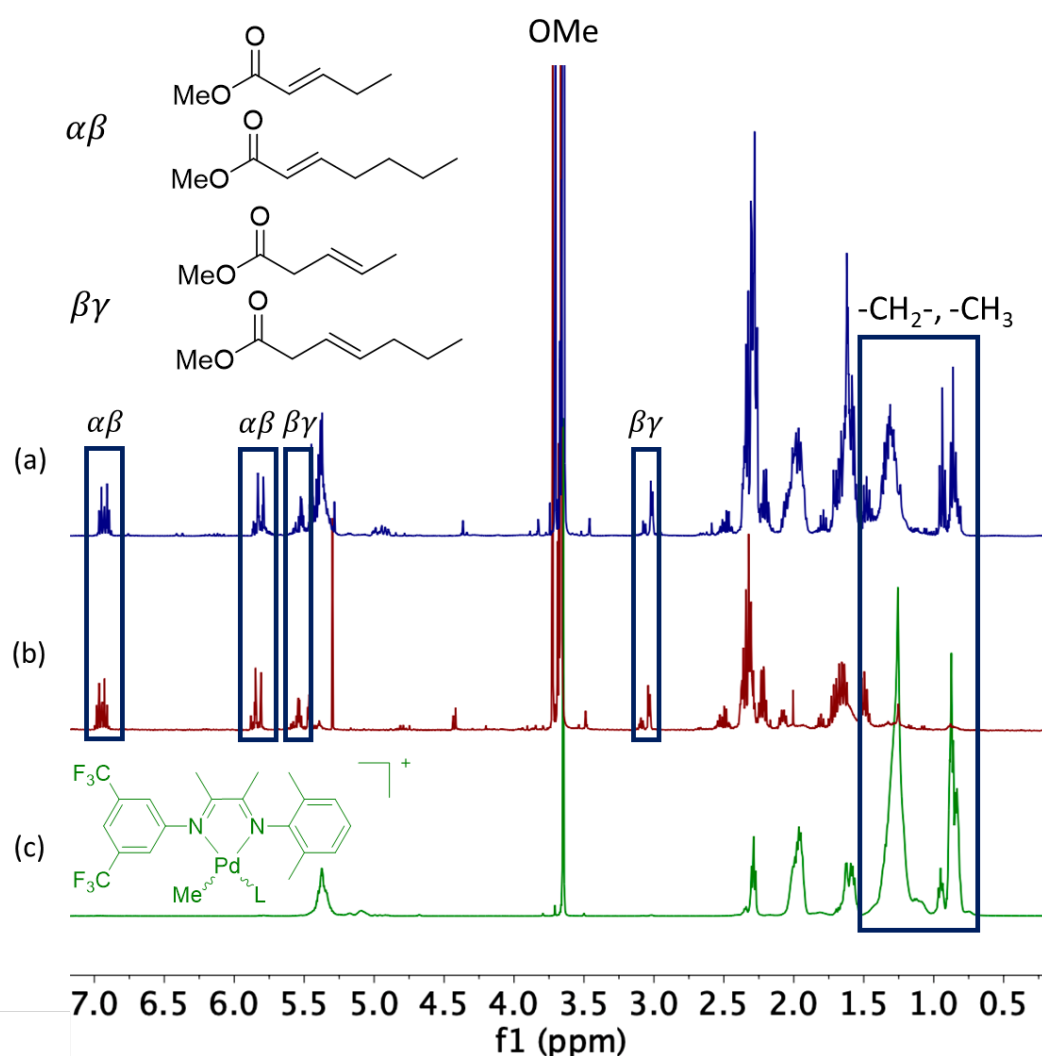

Fig. 2 ^{1}H NMR spectra (CDCl$_3$, 400 MHz, 298 K) of the dried residue of catalytic runs using: (a) complex **10**, (b) complex **9**; (c) complex [Pd(CH$_3$)(CH$_3$CN)(Ar,Ar'-DAB)][PF$_6$] from ref. 20 producing oligomeric material predominantly.

The slightly better performances of complex **10** prompted us to investigate the effect of reaction parameters, such as temperature, MA loading and ethylene pressure (Table 2). While some

caution must be exercised when interpreting the productivity values due to the small amounts of material formed, certain trends can be deduced. A 10 K increase in temperature gives an improved yield, however a Pd mirror was observed within 30 minutes, indicating a reduced stability of the catalytically active species under these conditions (entry 2). A decrease in [MA]/[Pd] ratio from 600 to 300 did not result in significant changes in productivity (26.6 *vs* 22.9 g P/g Pd, entry 3), suggesting no substantial inhibiting effect of the polar monomer. Increasing the ethylene pressure from 2.5 to 5.0 bar improves the yield by some 30%, but this trend is not linear, as the yield at 7.0 bar decreases substantially to about 60% with respect to the standard conditions (2.5 bar, entries 4,5). This intriguing fact has also been observed with catalysts containing different N-donor ligands that induce higher productivity, and it appears to be related to the fluorinated solvent.[19,33]

Table 2: **Optimisation of catalytic conditions using 10.**

Entry	Modification	Yield (mg)	Prod. (g P/g Pd)	Products GC-MS[a]
1	(standard conditions)	58.5	26.6	pentenoic (traces) and heptenoic esters
2	T = 318 K	74.8	33.7	butenes, hexenes, pentenoic (traces) and heptenoic esters
3	[MA]/[Pd] = 300	50.4	22.9	hexenes, pentenoic (traces) and heptenoic esters
4	$P_{ethylene}$ = 5.0 bar	74.8	34.0	butenes, hexenes, pentenoic and heptenoic esters
5	$P_{ethylene}$ = 7.0 bar	34.5	15.7	butenes, hexenes, pentenoic and heptenoic esters
6	no co-monomer	8.6	3.9	butenes, hexenes

Standard conditions: n_{Pd} = 21 μmol, 2,2,2-trifluoroethanol V = 21 mL, co-monomer = methyl acrylate (MA), [MA]/[Pd] = 600, T = 308 K, $P_{ethylene}$ = 2.5 bar, t = 18 h. [a] Products were also identified by NMR.

Reactivity studies

The data from this series indicate that increased steric bulk on the coordinating pyridine ring is detrimental to polymerisation, whereas the methyl substituent on the 3- position of the PYA ring allows some control relative to **9**. In order to gain further insight into the working mode of these complexes, stoichiometric NMR investigations were carried out by using both the most active complex **10** as well as the inactive complex **11** in the presence of either ethylene or MA only.

The reactivity of these complexes with MA in the absence of ethylene was investigated by following ^{1}H NMR spectra with time, at room temperature, using a 10 mM CD_2Cl_2 solution of the complex and 2 equivalents of the polar monomer. Fast methyl acrylate coordination to complex **10** and insertion into the Pd–Me bond is indicated by the disappearance of the Pd–Me signals (*cis* –0.05 ppm, *trans* 0.98 ppm), within 10 minutes (Fig. 3). The *cis* isomer reacts faster, since the integral ratio of these resonances drops from initially 6.5 to 1.7 after 1 min. In this spectrum, signals of a new species are evident (Fig. 3). Two-dimensional NMR characterisation by ^{1}H,^{1}H- and ^{1}H,^{13}C-correlation spectroscopy (Figures S17a,c) provided unambiguous evidence for the presence of a CH-CH$_2$-CH$_3$ fragment, whose protons are indicated as *c*, *b* and *a*, respectively (Fig. 3, Scheme 4). In addition, a cross peak between the methyl *a* signal and the resonance at 2.52 ppm attributed to the PYA C$_{PYA}$–Me group in the NOESY spectrum indicates that the latter is close in space to the CH-CH$_2$-CH$_3$ moiety, *i.e.* in mutual *cis* position (Fig. S17b). Further structural information was gained using low-temperature NMR experiments (Fig. S18). Thus, complex **10** and MA were mixed and allowed to react at room temperature for 1 min and cooled to 270 K in the NMR spectrometer. The 1D selective TOCSY showed that irradiation at any of the signals *a*, *b* or *c* with a mixing time of 80 ms returned the same spectrum consisting of only resonances due to *a*, *b* and *c*, indicating that they are all in the same spin system, thus confirming the CH-CH$_2$-CH$_3$ fragment (Fig. S18a). Furthermore, irradiation of signal *a* induced a weak NOE at the *b* and *c* signals, as well as the PYA methyl groups (both C–Me and N-Me, Figure S18b), in agreement with the *cis* configuration of this propyl fragment with the N$_{PYA}$ donor site deduced from room temperature 2D-NOESY analysis (Fig. S17b).
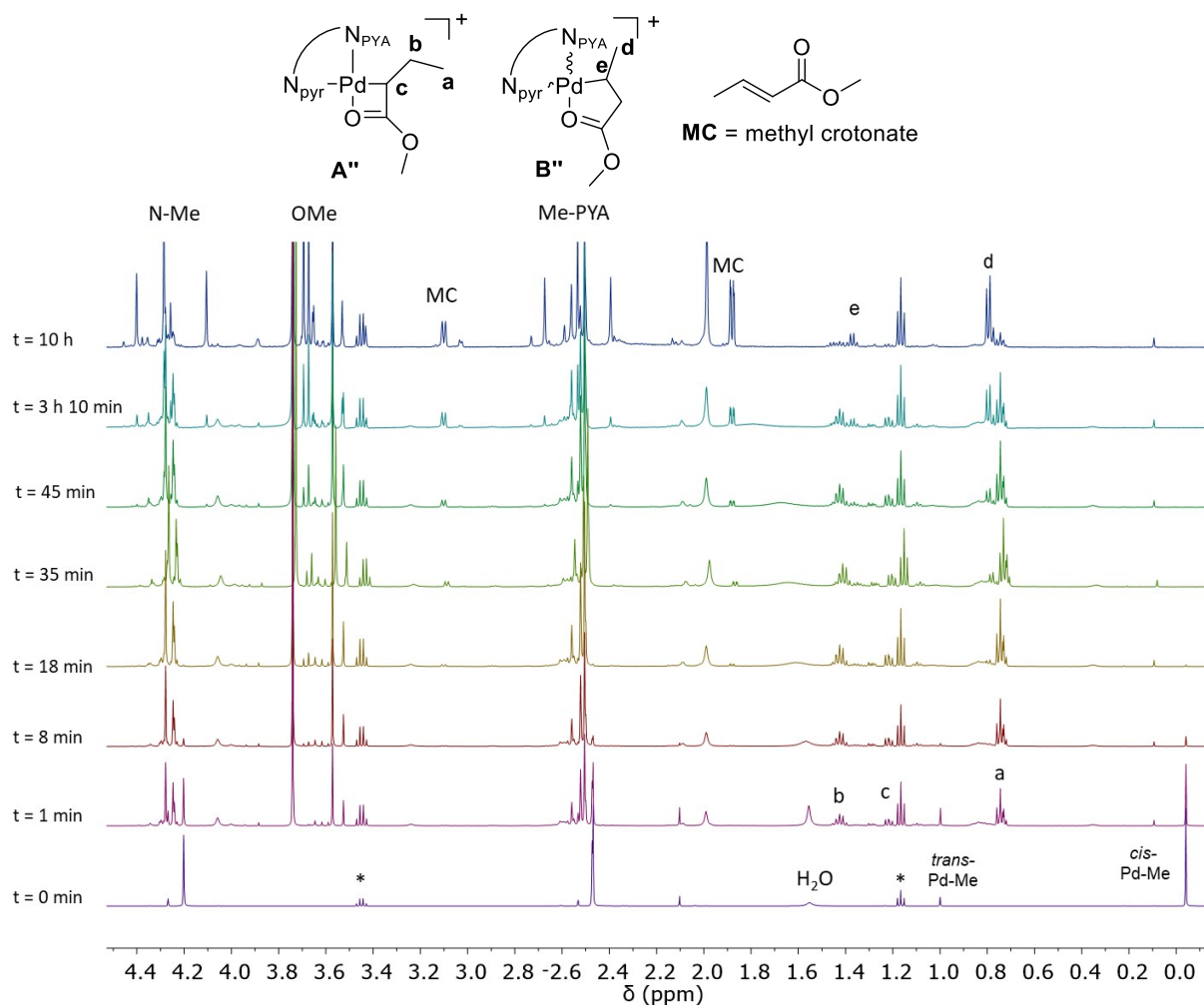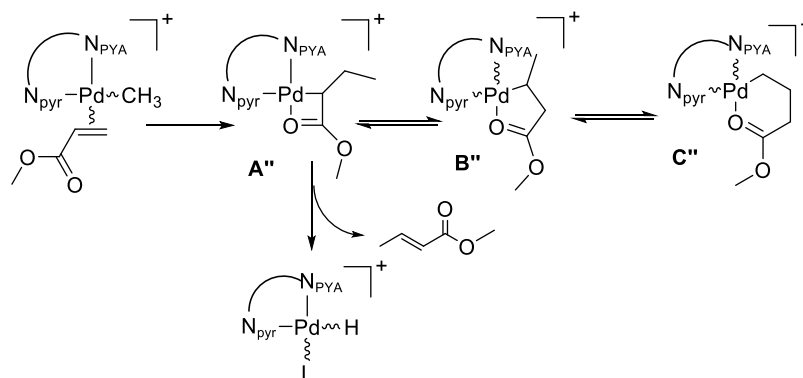
Fig. 3 Aliphatic region of ^{1}H NMR spectra (CD$_2$Cl$_2$, 500 MHz, 298 K) of reaction of complex **10** (10 mM) with MA (20 mM); * = diethyl ether.

Scheme 4 Proposed mechanism for the reaction of complex **10** with MA.

This detailed NMR analysis clearly indicates that the initial intermediate formed by the reaction of **10** with MA is the four-membered metallacycle **A''** (Fig. 3 and Scheme 4), originating from the regiospecific 2,1-migratory insertion of methyl acrylate into the Pd–Me bond to yield exclusively the *cis* isomer featuring the alkyl ligand adjacent to the N_{PYA} site. To the best of our knowledge, complex **A''** is the first example of such a 4-membered methyl acrylate adduct which is sufficiently stable to allow characterisation at room temperature. Allusion to **A''** as a transient species without full characterisation was made by Mecking *et al.* from in situ NMR investigation of the reactivity of a phosphino-sulfonato Pd–Me complex with MA.[34] In the case of Pd(II) complexes with α-diimine ligands, the **A''**-type four-membered metallacycle was detected only by NMR analysis at very low temperature (173 K) by Brookhart *et al.* and it displayed a $t_{1/2}$ of only 2 h at 193 K.[11,35] At higher temperatures (from 213 K to 253 K) it evolved to the **C''**-type six-membered palladacycle, which constitutes the usually observed species upon reacting either Pd–Me(Ar-DAB) or Pd–Me(Ar-BIAN) complexes with MA at room temperature.[19,20] This six-membered palladacycle **C''** has been demonstrated to be the resting state of the catalytic ethylene/MA copolymerisation cycle. During the preparation of this manuscript, a paper about a detailed NMR investigation of the reactivity of a Pd-Me complex featuring a peculiar, rigid and highly hindered α-diimine, with a broad scope of polar vinyl monomers, including methyl acrylate, appeared. Several palladacycle adducts were detected, but the 4-membered metallacycle was never observed.[36]

The stability of **A''** might be related to its stereochemistry that positions the Pd-alkyl moiety *cis* to the N_{PYA} fragment as the result of facile site epimerization taking place immediately after the methyl migratory insertion into the methyl acrylate. Our previous results suggest that β-hydride elimination is facile when the alkyl moiety resides *trans* to N_{PYA} fragment,[26] thus leading to the conclusion that for the reactivity of complex **10**, thanks to fast site epimerization, β-hydrogen elimination is slowed down as such to allow for the detection of **A''**.

The fate of **A''** was studied by following the evolution of the NMR spectra with time at room temperature. In the ^{1}H NMR spectrum at 18 min the signals of methyl crotonate begin to appear together with those of the **B''**-type five-membered palladacycle and they are the prevailing species present in the spectrum recorded at t = 10 h (Fig. 3). No resonances due to the six-membered metallacycle **C''** were observed.[19] These data therefore demonstrate that chain walking process on the Pd-PYA intermediate **A''** is very slow and is in competition with the associative displacement of methyl crotonate. The latter product might also form from **B''**, though the persistence of **B''** in the later-time NMR spectra indicates that methyl crotonate

elimination from **B''** is not very efficient (Scheme 4). The lack of productivity enhancement with lower [MA]/[Pd] ratio (*cf* Table 2) may therefore be due to the pronounced stability of the four-membered palladacycle.

The reactivity of **10** with ethylene was studied by saturating a 10 mM solution of the complex in CD_2Cl_2 for 10 min with the gaseous monomer and by analysing the evolving changes by ^{1}H NMR spectroscopy (Fig. 4). In agreement with our previous results on complex **9**,[26] the reaction of **10** with ethylene at room temperature is very fast. No signal of the precatalyst was present in the spectrum recorded immediately after saturation of the solution with ethylene (Figures 4, S20, S21). The observed resonances are due to propene, to *cis* and *trans*-2-butene and to the *trans*-$[Pd(CH_2CH_3)(PYA)(L)]^+$ intermediate (*trans*-Pd-Et), which was identified as the resting state of the catalytic cycle of ethylene dimerisation (Scheme 5).[26] These data indicate that the reactivity of **10** with ethylene follows the same pathway as proposed for complex **9**, that is, activation through migratory insertion of the alkene into the Pd–Me bond followed by β-hydrogen elimination with formation of propene and the Pd–H intermediate as the active species. Subsequent coordination-insertion of ethylene takes place leading to *cis*- and *trans*-Pd-ethyl intermediates: the former is active in the dimerisation reaction yielding *cis*- and *trans*-2-butene, while the latter is the dormant isomer of the catalyst (Scheme 5). These species were detected, at room temperature, for the first time by us, when complex **9** was the catalyst.[26] We demonstrated that the *cis*- isomer is the active species and the *trans*- one is the resting state together with a swap of the rate determining step from ethylene migratory insertion to *trans/cis* isomerisation of these intermediates depending on ethylene concentration. Consistent with these conclusions, recent NMR studies by Daugulis and Brookhart revealed that the *cis*/*trans* isomerisation rate is indeed dependent on the ethylene concentration.[37] In their system comprised of an anionic, electronically asymmetric N-O imine ligand, the isomerisation was determined to be much faster than the insertion step, which precluded any experimental assessment about which of the two isomers is preferably undergoing olefin insertion.[38]

Upon prolonged reaction time, broadening of the NMR signals due to complex decomposition was observed together with the appearance of a Pd mirror, as expected when ethylene concentrations become too low.
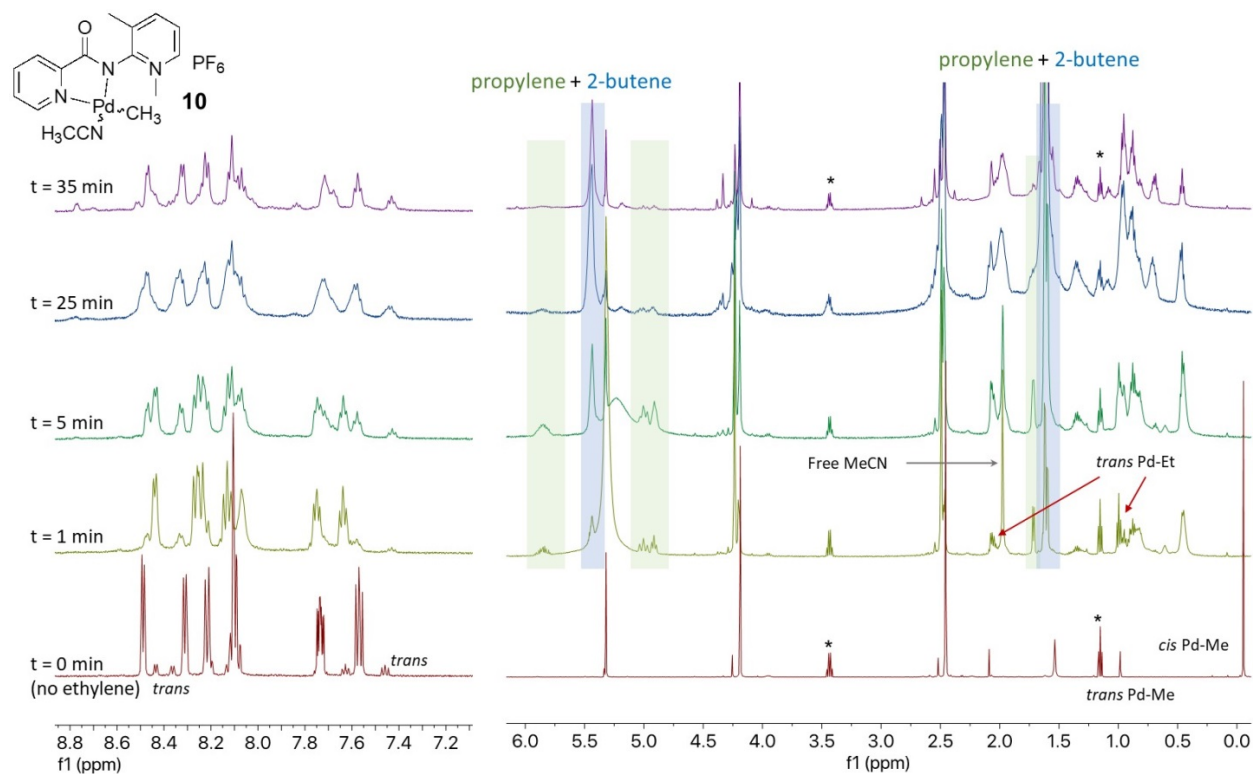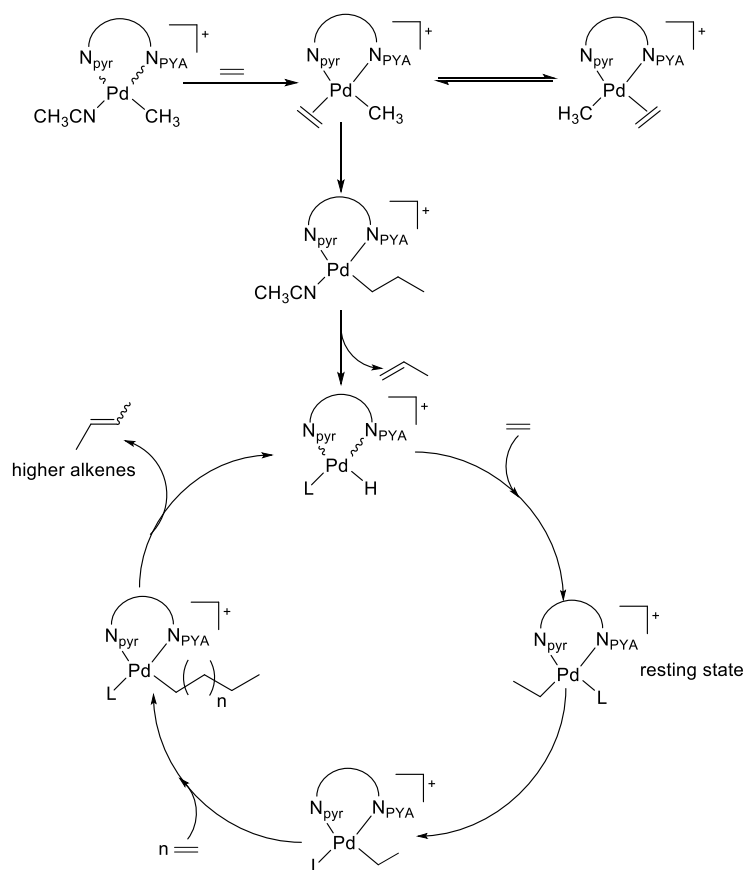
Fig. 4 Evolving changes in the ^{1}H NMR spectrum of **10** upon saturation with ethylene (CD$_2$Cl$_2$, 500 MHz, 298 K). * = diethyl ether.

Scheme 5 Proposed mechanism for the reaction of complex **10** with ethylene.

Combining these NMR investigations with the GC-MS data of the products of the catalytic runs, *viz.* formation of α,β- and β,γ-pentenoic and -heptenoic esters, allows for proposing a plausible mechanism (Scheme 6). Hence, the precatalyst is activated through migratory insertion of either ethylene or methyl acrylate into the Pd–Me bond leading to propene and methyl crotonate, respectively, together with the critical Pd-hydride intermediate. Since no methyl crotonate was found in the GC-MS analysis, and based on the time scale of reaction of the complex in the presence of only one monomer in NMR experiments, the insertion of ethylene is faster than that of the polar monomer under catalytic conditions and is therefore assumed to be the preferential activation pathway. In any case the active species is the Pd-hydride intermediate on which coordination-insertion of the alkene takes place leading to the Pd-ethyl complex which can follow two parallel pathways: *i)* coordination-insertion of methyl acrylate with formation of the four-membered palladacycle, similar to **A″**, followed by β-hydrogen elimination to yield α,β-pentenoic ester and recovering the active Pd–H species (Scheme 6, inner left cycle); or *ii)* coordination-insertion of a second molecule of ethylene, followed by coordination-insertion of methyl acrylate to afford the corresponding 4-membered palladacycle intermediate, from which β-hydrogen elimination yields α,β-heptenoic ester and again the Pd–H species (Scheme 6, inner right cycle). The remarkable stability of the four-membered palladacycle disfavours further monomer coordination reactions and hampers polymer chain growth, even at relatively low concentrations of the polar monomer. The unprecedented stability of the **A″** type intermediate also provides a rational for the low sensitivity of catalyst performance on the concentration of polar monomer (vide supra). In addition to these β-hydrogen elimination processes, the 4-membered palladacycle slowly evolves to the five-membered metallacycle from which both α,β-pentenoic and -heptenoic esters and the detected traces of the corresponding β,γ-isomers are obtained (Scheme 6, outer cycles).
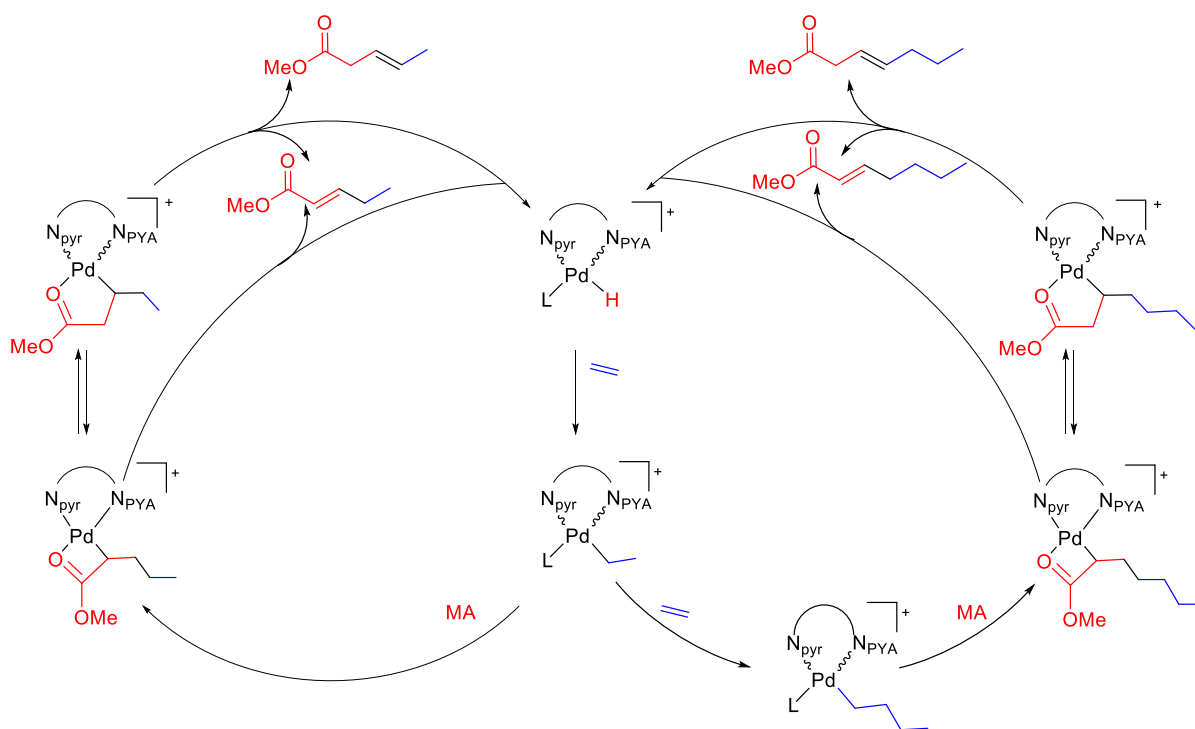
Scheme 6 Proposed mechanism for ethylene/MA coupling (left and right cycles for one and two ethylene insertions, respectively).

With the aim of elucidating the cause of the negligible productivity observed with the phenyl-substituted pyridine PYA complexes, the reactivity of methyl acrylate with complex **11** was investigated by *in situ* NMR spectroscopy (Fig. S22). The Pd–Me (0.06 ppm) and Pd–NCMe (1.69 ppm) signals in the ^{1}H NMR spectrum persisted longer than with **10**, dropping to approximately 50% of their original integration after 5 min (*cf* 65% of *cis* Pd–Me consumed from **10** already within 1 min). The formation of methyl crotonate together with the release of free ligand started to be observed at t = 10 min, yet no signal due to any of the three possible metallacycles is present (Fig. S22). These results indicate that the reactivity of **11** with MA is considerably slower than with **10**, and that β-hydrogen elimination occurs immediately after MA coordination-insertion. According to this model, the introduction of the phenyl group in position 6 of the pyridyl ring prevents both the efficient coordination of MA and the formation of the stable palladacycles required for propagation.

In addition, closer analysis of the ^{1}H NMR spectra from the reaction of MA with **11** showed the appearance of new signals in the aromatic region (multiplet at 7.2 ppm), whose intensity did not vary with time (Fig. S25) and hence suggested the formation of a stable species. The same signal was present in the ^{1}H NMR spectra of the catalytic products when complexes **11** or **12** were used as precatalysts (Fig. S23). Unambiguous characterisation of this new species

was achieved by X-ray diffraction analysis of single crystals grown from an acetonitrile solution of **11** which was kept in air exposed to solar light for 4 days. Under these conditions, the solution gradually turned from light yellow to orange and gave orange crystals of complex **13** containing a N_{PYA},N_{pyr},C_{Ph}-tridentate coordinated ligand due to cyclometallation of the phenyl substituent (Fig. 6). Bond lengths around the metal (Pd–N_{PYA} 2.146(2) Å, Pd–N_{pyr} 1.959(2), Pd–C 2.010(3) Å) are typical of previously reported bidentate PYA Pd complexes and of related C^N^N pincer complexes.[39] C–C bond lengths within the PYA ring range from 1.398(4) to 1.353(5) Å, indicating a mostly zwitterionic form due to the lack of apparent double bond localisation (see ESI for further details).
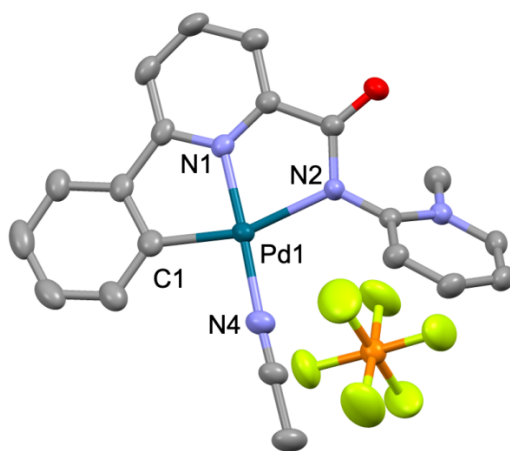

Fig. 6 ORTEP of complex **13** (50% probability thermal ellipsoids, H-atoms omitted for clarity). Selected bond lengths (Å): Pd1–N4 2.005(3), Pd1–C1 2.010(3), Pd1–N1 1.959(2), Pd1–N2 2.146(2); selected bond angles (°): N1–Pd1–N2 79.04(10), N1–Pd1–C1 81.11(12), N1–Pd1–N4 177.47(11), C1–Pd1–N2 160.04(12), N4–Pd1–C1 96.56(13), N4–Pd1–N2 103.26(11).

Monitoring the cyclometallation reaction by NMR spectroscopy revealed complete conversion within 60 min in pure MeCN (Fig. 7b), as indicated by the appearance of the signature cyclometallated phenyl multiplet at 7.2 ppm and free methane at 0.21 ppm. A control sample of **11** which was excluded from light showed no change during the same experiment (Fig. 7a), indicating that this transformation is indeed photochemically induced.[40] Irradiation of a sample of **11** in MeCN with UV light to steady state (60 min) again yielded an orange solution. Comparison of the UV-vis absorption spectra of the solution before and after irradiation show a more structured absorption profile after irradiation (Fig. S24), consistent with a loss of rotation due to cyclometallation. Similar cyclometallation reactions resulting from C–H bond activation of alkyl substituents in *ortho*-positions of N-donor ligands present in Pd(II) complexes were previously reported.[41-45]

We note that complex **13** is, unsurprisingly, catalytically inactive (Fig. S26). In catalytic polymerisation experiments, this complex is formed at early stages, and subsequently its concentration does not vary, which suggests that the cyclometallation is an off-cycle process of the catalyst precursor and not an on-cycle catalyst deactivation pathway.
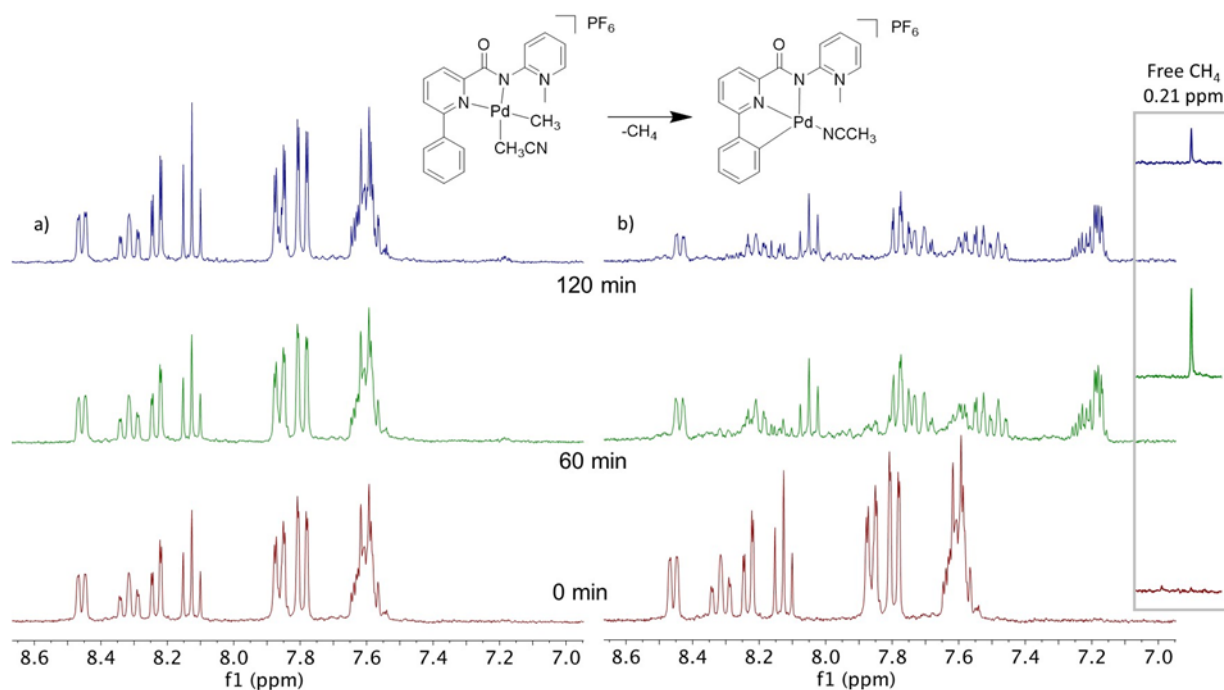

Fig. 7 ^{1}H NMR spectra (CD$_3$CN, 300 MHz, 298 K) of the evolution over time of **11**: a) in the dark (no change); b) under UV irradiation (formation of **13**).

Conclusion

Modulation of our previously published pyridyl-PYA palladium catalyst **9** at the PYA fragment successfully decelerates the rate of β-hydride elimination during MA/ethylene copolymerisation to facilitate the production of oligomeric species. While productivity remains low, the high propensity of this catalyst system towards MA incorporation is preserved when considering the formation of pentenoic and heptanoic esters as major products. While the increased steric bulk at the PYA side efficiently enhances the kinetics of olefin insertion *vs* β-H elimination, this modification also promotes a remarkable persistence of the unusual 4-membered **A''**-type palladacycle intermediate. The stability of this intermediate may prevent further olefin insertion and polymer growth. This work further demonstrates the deleterious effect of increased steric bulk on the coordinating pyridine ring, revealing degradation of the pre-catalyst due to its sensitivity towards light and ensuing UV-induced cyclometallation. These data offer a useful roadmap for further tailoring of these versatile PYA systems towards efficient copolymerisation catalysis.

Experimental

All complexes were synthesised under exclusion of air using standard Schlenk techniques under an atmosphere of dry nitrogen unless otherwise stated. All starting materials and reagents were obtained from commercial sources and used as received. NMR spectra were recorded either on a Varian 500 MHz spectrometer or a Bruker spectrometer operating at 300 MHz. Chemical shifts δ are reported in ppm (J in Hz) relative to residual protic solvents. Irradiation of complexes was carried out using a UVP "Blak-Ray" B-100AP 100 W 365 nm lamp.

General Procedure for the Formation of Amides 2 and 3.

Picolinic acid (1.231 g, 10 mmol) was refluxed in $SOCl_2$ (10 mL, 0.14 mol) for 3 h under an N_2 atmosphere. $SOCl_2$ was removed under reduced pressure and the residue was dissolved in dry THF (40 mL). This solution was transferred *via* cannula to a solution of the corresponding aminopyridine (10 mmol) in THF (50 mL), followed by NEt_3 (2.5 mL, 18 mmol). The mixture was refluxed for 48 h, filtered, and the solvent was removed under reduced pressure. The brown solid residue was purified by column chromatography (SiO_2) using a gradient pentane ethyl acetate eluent to yield the pure products as white solids.

N-(3-Methylpyridin-2-yl)picolinamide (2). ^{1}H NMR (300 MHz, CDCl₃) δ 10.18 (s, 1H N-H), 8.63 (ddd, J = 4.8, 1.6, 0.9 Hz, 1H), 8.36 (dd, J = 4.8, 1.3 Hz, 1H), 8.31 (dt, J = 7.9, 1.0 Hz, 1H), 7.90 (td, J = 7.7, 1.7 Hz, 1H), 7.59 (dd, J = 7.5, 0.9 Hz, 1H), 7.49 (ddd, J = 7.6, 4.8, 1.2 Hz, 1H), 7.11 (dd, J = 7.5, 4.8 Hz, 1H), 2.39 (s, 3H) ppm. ^{13}C NMR (75 MHz, CDCl₃) δ 162.21, 149.84, 149.54, 148.28, 146.46, 139.71, 137.68, 127.32, 126.74, 122.80, 121.49, 77.58, 77.16, 76.74, 18.25 ppm. HRMS: calc. for $C_{12}H_{12}N_3O$ [M+H⁺]: 214.0977 m/z Found: 214.09755 m/z.

6-Phenyl-*N*-(pyridin-2-yl)picolinamide (3). ^{1}H NMR (300 MHz, CDCl₃) δ 10.49 (s, 1H), 8.39 (d, J = 8.4 Hz, 1H), 8.31 (dd, J = 4.9, 1.0 Hz, 1H), 8.15 (dd, J = 7.1, 1.6 Hz, 1H), 8.04 – 7.95 (m, 2H), 7.93 – 7.79 (m, 2H), 7.74 – 7.63 (m, 1H), 7.49 – 7.33 (m, 3H), 7.00 (ddd, J = 7.3, 4.9, 0.9 Hz, 1H) ppm. ^{13}C NMR (75 MHz, CDCl₃) δ 162.80, 156.30, 151.25, 149.18, 148.27, 138.54, 138.44, 137.92, 129.75, 129.02, 127.15, 123.64, 121.01, 120.03, 114.16, 77.58, 76.74 ppm. HRMS: calc. for $C_{17}H_{14}ON_3$ [M+H] ⁺: 276.1131 m/z Found: 276.1124 m/z.

N-(3-Methylpyridin-2-yl)-6-phenylpicolinamide (4). ^{1}H NMR (300 MHz, CDCl₃) δ 10.36 (s, 1H), 8.39 (dd, J = 4.8, 1.2 Hz, 1H), 8.27 (dd, J = 7.1, 1.6 Hz, 1H), 8.13 – 8.04 (m, 2H), 8.04

– 7.90 (m, 2H), 7.63 (dd, J = 7.5, 0.9 Hz, 1H), 7.56 – 7.45 (m, 3H), 7.14 (dd, J = 7.5, 4.8 Hz, 1H), 2.43 (s, 3H). ^{13}C NMR (75 MHz, CDCl$_3$) δ 162.26, 156.23, 149.55, 146.35, 139.92, 138.64, 138.28, 129.75, 129.07, 127.52, 127.14, 123.61, 121.56, 121.23, 18.34. HRMS: calc. for C$_{18}$H$_{16}$ON$_3$ [M+H$^+$]: 290.1288 m/z Found: 290.1287 m/z.

General Procedure for the Synthesis of Pyridinium Salts. The corresponding amide (2.0 mmol) were dissolved in MeCN (15 mL) in a pressure tube. MeI (187 μL, 3.0 mmol) was added, and the reaction mixture was stirred for 18 h at 80 °C. The solution was cooled to room temperature and concentrated to 5 mL. Et$_2$O (50 mL) was added, and the formed yellow precipitate was filtered and washed with cold Et$_2$O to yield the compounds as yellow solids.

1,3-Dimethyl-2-(picolinamido)pyridin-1-ium iodide (6). ^{1}H NMR (300 MHz, DMSO) δ 11.63 (s, 1H, NH), 9.03 (d, J = 5.8 Hz, 1H, CH$_{PYA}$), 8.84 (d, J = 4.6 Hz, 1H), CH$_{Pyr}$, 8.64 (d, J = 7.8 Hz, 1H, CH$_{PYA}$), 8.25 – 8.10 (m, 2H, 2CH$_{Pyr}$), 8.06 (dd, J = 7.9, 6.2 Hz, 1H, CH$_{PYA}$), 7.88 – 7.75 (m, 1H, CH$_{Pyr}$), 4.27 (s, 3H, N-Me), 2.40 (s, 3H, -Me) ppm. ^{13}C NMR (75 MHz, DMSO) δ 163.44, 148.99 (CH$_{Pyr}$), 148.15 (CH$_{PYA}$), 147.51 (), 144.78 (CH$_{PYA}$), 138.52, 137.32, 128.23, 125.50, 123.25, 116.99, 44.87, 17.34 ppm. HRMS: calc. for C$_{13}$H$_{14}$N$_3$ONa [M + Na]$^+$ 228.1122 m/z found 228.1131 m/z.   EA: Anal. calc. for C$_{13}$H$_{14}$N$_3$OI: %C 43.96, %H 3.97, %N 11.83, found: %C 44.05, %H 3.86, %N 11.43

1-Methyl-2-(6-phenylpicolinamido)pyridin-1-ium iodide (7). ^{1}H NMR (300 MHz, DMSO) δ 11.43 (s, 1H), 9.05 (d, J = 5.4 Hz, 1H), 8.72 – 8.63 (m, 1H), 8.55 (dd, J = 8.4, 1.0 Hz, 1H), 8.41 (dd, J = 7.5, 1.3 Hz, 1H), 8.35 (dd, J = 8.0, 1.4 Hz, 2H), 8.27 (t, J = 7.6 Hz, 1H), 8.22 (dd, J = 7.6, 1.3 Hz, 1H), 8.00 – 7.87 (m, 1H), 7.68 – 7.47 (m, 3H), 4.44 (s, 3H) ppm. ^{13}C NMR (75 MHz, DMSO) δ 162.63, 155.54, 147.09, 146.98, 146.49, 145.37, 139.92, 136.92, 130.09, 129.06, 127.16, 124.92, 123.16, 122.40, 121.77, 43.92 ppm. HRMS: calc. for C$_{18}$H$_{16}$ON$_3$ [M]$^+$ 290.1288 m/z found 290.1278 m/z. EA: Anal. calc. for C$_{19}$H$_{15}$N$_3$OI: %C 51.20, %H 3.63, %N 10.10, found: %C 51.20, %H 3.77, %N 10.02

1,3-Dimethyl-2-(6-phenylpicolinamido)pyridin-1-ium iodide (8). ^{1}H NMR (300 MHz, DMSO) δ 11.32 (s, 1H), 9.08 (d, J = 5.7 Hz, 1H), 8.68 (d, J = 7.8 Hz, 1H), 8.43 – 8.34 (m, 3H), 8.22 (t, J = 7.8 Hz, 1H), 8.17 – 8.06 (m, 2H), 7.62 – 7.49 (m, 3H), 4.33 (s, 3H), 2.46 (s, 3H).

^{13}C NMR (75 MHz, DMSO) δ 163.37, 155.66, 148.20, 147.32, 146.19, 144.81, 139.55, 137.54, 137.03, 129.98, 128.89 (2C), 127.21 (2C), 125.68, 124.43, 121.65, 45.01, 17.40. HRMS: calc. for $C_{19}H_{18}ON_3$ [M - I]$^+$ 304.1444 m/z found 304.1433 m/z. EA: Anal. calc. for $C_{19}H_{18}N_3OI$: %C 52.91, %H 4.21, %N 9.74, found: %C 52.72, %H 4.15, %N 9.65

[Pd(5)(Me)(MeCN)](PF$_6$) (9). Pyridinium **5** (0.175 g, 0.514 mmol) was dissolved in a water:methanol mixture (2 mL, 1:1). This solution was filtered and a saturated methanolic solution of NH$_4$PF$_6$ was added dropwise, resulting in a thick white precipitate which was collected by filtration and washed with copious amounts of water to yield the corresponding PF$_6$ salt of **5** as a white solid (0.164 g, 89%). This salt (81 mg, 0.23 mmol) and K$_2$CO$_3$ (0.1 g, excess) were stirred in dry CH$_2$Cl$_2$ (5 mL) for 20 min. Then [Pd(cod)(Me)Cl] (59 mg, 0.23 mmol) was added and the solution stirred at room temperature for 3 h. The precipitate was filtered out and the yellow filtrate was dried *in vacuo*, redissolved in CH$_2$Cl$_2$ (1 mL), triturated with Et$_2$O and filtered to give [Pd(5)(Me)Cl] as bright yellow solid which was used for the next step without further purification (77 mg, 0.21 mmol). [Pd(5)(Me)Cl] (37 mg, 0.10 mmol) was stirred at room temperature with NH$_4$PF$_6$ (20 mg, 0.12 mmol) in dry acetonitrile (5 mL) for 2.5 h. A white precipitate of NH$_4$Cl was observed. The solution was allowed to stand in the refrigerator for 20 min to allow full precipitation and was then filtered through Celite. The solvent was removed *in vacuo* and cold, dry CH$_2$Cl$_2$ (<5 mL) was added to the resulting solid. The suspension was filtered through Celite and the volume of the solution was reduced *in vacuo* to *ca.* 1 mL. The product **9** was precipitated by trituration in cold Et$_2$O, filtered and dried *in vacuo* and was isolated as a white solid (47 mg, 91%, consisting of about 60% *cis* and 40% *trans* complex. All spectroscopic properties are identical to those previously published.[31]

[Pd(6)(Me)(MeCN)](PF$_6$) (10)
[Pd(Me)Cl(cod)] (71.7 mg, 0.27 mmol), the pyridinium salt **6** (90.4 mg, 0.26 mmol) and K$_2$CO$_3$ (70.1 mg, 0.51 mmol) were stirred in dry MeCN (3 mL) under N$_2$. The flask was protected from light and AgPF$_6$ (0.14 g, 0.56 mmol) was transferred to the vial using additional dry MeCN (10 mL). After 5 h, the solvent was evaporated under reduced pressure and the residue was dissolved in CHCl$_3$ (5 mL). The resulting suspension was filtered through a pad of Celite, its volume reduced *in vacuo* and pentane added to precipitate the product as an off white solid (111 mg, 77 %; *ca.* 6:1 *cis*:*trans*). HRMS: calc. for $C_{16}H_{19}ON_4Pd$ [M $-$ PF$_6$]$^+$ 389.0594 m/z found 389.0588 m/z.

Spectroscopic data of the *cis* isomer (86%): ^{1}H NMR (300 MHz, CD_2Cl_2) δ 8.50 (d*pt*, $J = 5.2$, 1.1 Hz, 1H, CH_{Pyr}), 8.31 (d, $J = 6.0$ Hz, 1H, CH_{PYA}), 8.22 (d, $J = 7.7$ Hz, 1H, CH_{Pyr}), 8.14 – 7.98 (m, 2H, 2CH_{Pyr}), 7.73 (*ptd*, $J = 5.2$, 3.4 Hz, 1H, CH_{Pyr}), 7.57 (dd, $J = 7.8$, 6.3 Hz, 1H, CH_{PYA}), 4.18 (s, 3H, N-CH_3), 2.45 (br. s, 6H, Pd-CH_3CN + $CH_{3\ PYA}$), -0.05 (s, 3H, Pd-CH_3) ppm. ^{13}C NMR (75 MHz, CD_2Cl_2) δ 150.2 (C_q), 148.4 (CH_{Pyr}), 146.7 (CH_{PYA}), 141.9 (CH_{PYA}), 140.2 (CH_{Pyr}), 138.0 (C_q), 129.1 (CH_{Pyr}), 125.8 (CH_{Pyr}), 123.2 (CH_{PYA}), 44.7 (N-CH_3), 18.4 ($CH_{3\ PYA}$), 3.9 ($CH_{3\ PYA}$), -6.5 (Pd-CH_3) ppm.

Selected spectroscopic data of the *trans isomer* (*ca.* 14 %): ^{1}H NMR (300 MHz, CD_2Cl_2) δ 8.44 (d, $J = 6.0$ Hz, 1H), 8.36 (d, $J = 7.6$ Hz, 1H), 7.63 (m, 1H), 7.46 (*pt*, $J = 7.0$ Hz, 1H) 4.25 (s, 3H, N-CH_3), 2.52 (s, 3H, $CH_{3\ PYA}$), 2.08 (s, 3H, Pd-CH_3CN), 0.98 (s, 3H, Pd-CH_3) ppm. No ^{13}C NMR data available due to low concentration.

[Pd(7)(Me)(MeCN)](PF$_6$) (11)

According to the procedure described for complex **10** starting from [Pd(Me)Cl(cod)] (64.0 mg, 0.24 mmol), pyridinium salt **7** (105.0 mg, 0.25 mmol), K_2CO_3 (69.0 mg, 0.50 mmol) and AgPF$_6$ (132.8 g, 0.53 mmol). The title product was obtained as an off-white solid as a single isomer (*cis* only, 118 mg, 79% yield).

^{1}H NMR (300 MHz, CD_2Cl_2) δ 8.47 (dd, $J = 6.4$, 1.7 Hz, 1H, CH_{PYA}), 8.31 (*ptd*, $J = 8.2$, 1.7 Hz, 1H, CH_{PYA}), 8.23 (dd, $J = 7.7$, 1.4 Hz, 1H, CH_{Pyr}), 8.12 (*pt*, $J = 7.7$ Hz, 1H, CH_{Pyr}), 7.86 (dd, $J = 8.0$, 1.6 Hz, 2H, CH_{Ph}), 7.79 (m, 2H, CH_{PYA} + CH_{Pyr}), 7.61 (m, 4H, 3CH_{Ph} + CH_{PYA}), 4.31 (s, 3H, N-CH_3), 1.69 (s, 3H, Pd-CH_3CN), 0.06 (s, 3H, Pd-CH_3) ppm. ^{13}C NMR (75 MHz, CD_2Cl_2) δ 171.1 (C=O), 160.3 (C_q), 160.1 (C_q), 152.6 (C_q), 145.3 (CH_{PYA}), 144.6 C_q, 144.1 (CH_{PYA}), 140.2 (CH_{Pyr}), 139.7 (C_q), 130.5 (CH_{Ph}), 130.0 (2CH_{Ph}), 129.3 (2CH_{Ph}), 129.0 (CH_{Pyr} or CH_{PYA}), 129.0 (CH_{Pyr} or CH_{PYA}), 124.4 (CH_{Pyr}), 122.8 (CH_{PYA}), 44.6 (N-CH_3), 3.4 (Pd-$NCCH_3$), -3.7 (Pd-CH_3) ppm. HRMS: *m/z* calc. for $C_{21}H_{21}N_4OPd$ [M – PF$_6$]$^+$ 451.0745, found 451.0726; *m/z* calc. for $C_{18}H_{14}N_3OPd$ [M – CH_4 – MeCN – PF$_6$] 394.0172 m/z found 394.0157.

[Pd(8)(Me)(MeCN)](PF$_6$) (12)

According to the procedure described for complex **10**, reaction of [Pd(Me)Cl(cod)] (64.5 mg, 0.24 mmol), the pyridinium salt **8** (103.9 mg, 0.24 mmol), K_2CO_3 (67.7 mg, 0.49 mmol), and AgPF$_6$ (130.6 g, 0.52 mmol) yielded complex **12** as an orange-white solid as a single isomer (*cis* only, 106 mg, 72% yield).

^{1}H NMR (300 MHz, CD$_2$Cl$_2$) δ 8.37 (br. d, J = 6.3 Hz, 1H, CH$_{PYA}$), 8.29 – 8.16 (m, 2H, CH$_{PYA}$ + CH$_{Pyr}$), 8.12 (pt, J = 7.7 Hz, 1H, CH$_{Pyr}$), 7.83 (m, 2H, 2CH$_{Ph}$), 7.78 (dd, J = 7.7, 1.5 Hz, 1H, CH$_{Pyr}$), 7.65 – 7.51 (m, 4H, 3CH$_{Ph}$ + CH$_{PYA}$), 4.25 (s, 3H, N-CH$_3$), 2.51 (s, 3H, CH$_{3\ PYA}$), 1.70 (s, 3H, Pd-NCCH$_3$), -0.07 (s, 3H, Pd-CH$_3$) ppm. ^{13}C NMR (75 MHz, CD$_2$Cl$_2$) δ 167.4 (C=O), 157.6 (C$_q$), 149.4 (C$_q$), 143.9 (CH$_{PYA}$), 139.3 (CH$_{PYA}$), 137.4 (CH$_{Pyr}$), 137.0 (C$_q$), 135.3 (C$_q$), 127.6 (CH$_{Ph}$), 127.3 (2CH$_{Ph}$), 126.5 (2CH$_{Ph}$), 126.4 (CH$_{Pyr}$), 121.5 (CH$_{Pyr}$), 120.3 (CH$_{PYA}$), 42.0 (N-CH$_3$), 15.7 (CH$_{3\ PYA}$), 0.6 (Pd-NCCH$_3$), -7.3 (Pd-CH$_3$) ppm (some quaternary carbons unresolved). HRMS: calc. for C$_{19}$H$_{16}$N$_{30}$Pd [M – CH$_4$ – MeCN – PF$_6$]$^+$ 408.0334 m/z found 408.0318.

[Pd(N$_{PYA}$,N$_{pyr}$,C$_{Ph}$)(MeCN)](PF$_6$) (13). Irradiation of a MeCN solution (0.7 mL) of **11** (7.2 mg, 0.012 mmol) in a NMR tube with a UV lamp afforded complex **13** in quantitative yields by UV-vis and NMR spectroscopy.

^{1}H NMR (300 MHz, CD$_3$CN) δ 8.39 (dd, J = 6.4, 1.7 Hz, 1H, CH$_{PYA}$), 8.30 – 8.18 (m, 1H, CH$_{PYA}$), 8.15 – 8.04 (m, 1H, , CH$_{Pyr}$), 7.87 (dd, J = 8.1, 1.2 Hz, 1H, CH$_{Pyr}$), 7.72 (ddd, J = 8.1, 6.4, 1.3 Hz, 2H, , CH$_{PYA}$, CH$_{Pyr}$), 7.65 – 7.57 (m, 1H, , CH$_{Ph(cyclo)}$), 7.50 (ddd, J = 7.7, 6.4, 1.5 Hz, 1H, CH$_{PYA}$), 7.30 – 7.04 (m, 2H, CH$_{Ph(cyclo)}$), 4.13 (s, 3H, N-CH$_3$), 2.15 (s, 3H, Pd-NCCH$_3$). ^{13}C NMR (75 MHz, CD$_3$CN) δ 169.3 (C$_q$), 165.5 (C$_q$), 154.0 (C$_q$), 152.5 (C$_q$), 147.0 (C$_q$), 145.5 (CH$_{PYA}$), 144.6 (CH$_{PYA}$), 142.1 (CH$_{Pyr}$), 135.5 (CH$_{Ph}$), 131.5 (CH$_{Ph}$), 129.6 (C–Pd) 126.8 (CH$_{PYA/Pyr}$), 126.8 (CH$_{Ph}$), 125.7 (CH$_{Ph}$), 123.3, 122.2, 121.7, 118.3, 44.5 (N-CH$_3$) ppm. HRMS: calc. for C$_{20}$H$_{17}$N$_4$OPd [M – PF$_6$] 435.0437 m/z, found 435.0423 m/z.

Ethylene/Methyl acrylate (MA) cooligomerisation reactions. All catalytic experiments were performed using a Büchi "tinyclave" glass reactor equipped with an interchangeable 50 mL glass vessel. The vessel was loaded with the desired complex (21 μmol), TFE (21 mL), and MA (1.13 mL). The reactor was then placed in a preheated oil bath and connected to the ethylene tank. Ethylene was bubbled for 10 min, and the reactor was pressurised. The reaction mixture was stirred at constant temperature and pressure. After the appropriate time, the reactor was cooled to RT and vented. An aliquot (200 μL) of the reaction mixture was withdrawn and diluted in MeOH (1 mL) for GC-MS analysis. No separation of palladium black was performed. The reaction mixture was poured into a 50 mL round-bottomed flask with the CH$_2$Cl$_2$ (3 x 1 mL) used to wash the glass vessel. Volatiles were removed under reduced pressure, and the residue was dried to constant weight and analysed by using NMR spectroscopy.

Qualitative analysis of the low molecular weight products of co-oligomerisation was conducted by GC-MS using an Agilent GC 7890 instrument coupled with a 5975 MSD. Separation of the products was obtained using a DB-225 ms column (J&W, 60 m, 0.25 mm ID, 0.25 mm film) with He as carrier. Before analysis, samples were diluted with methanol.

In situ NMR experiments with ethylene. Ethylene was bubbled for 10 min to a 10 mM solution of palladium complexes **10** or **11** in CD_2Cl_2 in an NMR tube. Then, ^1H NMR spectra were recorded at 298 K immediately after and at selected times.

In situ NMR experiments with MA. To a 10 mM solution of palladium complexes **10** or **11** in CD_2Cl_2 in an NMR tube, 2 equivalents of MA were added at 298 K. Then, ^1H NMR spectra were recorded at 298 K immediately after and at selected times.

For the low temperature experiments, the tube was cooled to 270 K. NOESY experiments were performed using the standard parameters and a mixing time of 500 ms.

There are no conflicts to declare.

Electronic Supplementary Information (ESI): NMR analyses of ligand precursors, complexes and catalytic products, catalytic optimisation results, spectroscopic data for the formation of **13**, and crystallographic details.

References

1.   L. S. Boffa and B. M. Novak, *Chem. Rev.*, 2000, **100**, 1479-1494.
2.   A. Nakamura, S. Ito and K. Nozaki, *Chem. Rev.*, 2009, **109**, 5215-5244.
3.   A. Berkefeld and S. Mecking, *Angew. Chem. Int. Ed.*, 2008, **47**, 2538-2542.
4.   J.-Y. Dong and Y. Hu, *Coord. Chem. Rev.*, 2006, **250**, 47-65.
5.   B. P. Carrow and K. Nozaki, *Macromolecules*, 2014, **47**, 2541-2555.
6.   C. Chen, *Nat. Rev. Chem.*, 2018, **2**, 6-14.
7.   A. Keyes, H. E. Basbug Alhan, E. Ordonez, U. Ha, D. B. Beezer, H. Dau, Y.-S. Liu, E. Tsogtgerel, G. R. Jones and E. Harth, *Angew. Chem. Int. Ed.*, 2019, **58**, 12370-12391.
8.   L. K. Johnson, C. M. Killian and M. Brookhart, *J. Am. Chem. Soc.*, 1995, **117**, 6414-6415.

9.   S. D. Ittel, L. K. Johnson and M. Brookhart, *Chem. Rev.*, 2000, **100**, 1169-1204.
10.   L. K. Johnson, S. Mecking and M. Brookhart, *J. Am. Chem. Soc.*, 1996, **118**, 267-268.
11.   S. Mecking, L. K. Johnson, L. Wang and M. Brookhart, *J. Am. Chem. Soc.*, 1998, **120**, 888-899.
12.   Z. Chen and M. Brookhart, *Acc. Chem. Res.*, 2018, **51**, 1831-1839.
13.   L. Guo, W. Liu and C. Chen, *Mater. Chem. Front.*, 2017, **1**, 2487-2494.
14.   F. Wang and C. Chen, *Polym. Chem.*, 2019, **10**, 2354-2369.
15.   E. Drent, R. van Dijk, R. van Ginkel, B. van Oort and R. I. Pugh, *Chem. Commun.*, 2002, 744-745.
16.   A. Nakamura, T. M. J. Anselment, J. Claverie, B. Goodall, R. F. Jordan, S. Mecking, B. Rieger, A. Sen, P. Van Leeuwen and K. Nozaki, *Accounts of Chemical Research*, 2013, **46**, 1438-1449.
17.   J. A. Gladysz, Z. T. Ball, G. Bertrand, S. A. Blum, V. M. Dong, R. Dorta, F. E. Hahn, M. G. Humphrey, W. D. Jones, J. Klosin, I. Manners, T. J. Marks, J. M. Mayer, B. Rieger, J. C. Ritter, A. P. Sattelberger, J. M. Schomaker and V. W.-W. Yam, *Organometallics*, 2012, **31**, 1-18.
18.   C. Tan and C. Chen, *Angew. Chem. Int. Ed.*, 2019, **58**, 7192-7200.
19.   A. Meduri, T. Montini, F. Ragaini, P. Fornasiero, E. Zangrando and B. Milani, *ChemCatChem*, 2013, **5**, 1170-1183.
20.   V. Rosar, T. Montini, G. Balducci, E. Zangrando, P. Fornasiero and B. Milani, *ChemCatChem*, 2017, **9**, 3402-3411.
21.   S. Dai, S. Zhou, W. Zhang and C. Chen, *Macromolecules*, 2016, **49**, 8855-8862.
22.   F. Zhai, J. B. Solomon and R. F. Jordan, *Organometallics*, 2017, **36**, 1873-1879.
23.   G. Canil, V. Rosar, S. Dalla Marta, S. Bronco, F. Fini, C. Carfagna, J. Durand and B. Milani, *ChemCatChem*, 2015, **7**, 2255-2264.
24.   V. Rosar, D. Dedeic, T. Nobile, F. Fini, G. Balducci, E. Alessio, C. Carfagna and B. Milani, *Dalton Trans.*, 2016, **45**, 14609-14619.
25.   A. Dall'Anese, M. Fiorindo, D. Olivieri, C. Carfagna, G. Balducci, E. Alessio, J. Durand and B. Milani, *Macromolecules*, 2020, **53**, 7783-7794.
26.   M. Navarro, V. Rosar, T. Montini, B. Milani and M. Albrecht, *Organometallics*, 2018, **37**, 3619-3630.
27.   M. Navarro, C. A. Smith and M. Albrecht, *Inorg. Chem.*, 2017, **56**, 11688-11701.
28.   M. Navarro, M. Li, S. Bernhard and M. Albrecht, *Dalton Trans.*, 2018, **47**, 659-662.
29.   K. F. Donnelly, C. Segarra, L.-X. Shao, R. Suen, H. Müller-Bunz and M. Albrecht, *Organometallics*, 2015, **34**, 4076-4084.
30.   V. Leigh, D. J. Carleton, J. Olguin, H. Mueller-Bunz, L. J. Wright and M. Albrecht, *Inorg. Chem.*, 2014, **53**, 8054-8060.
31.   A. Scarel, J. Durand, D. Franchi, E. Zangrando, G. Mestroni, B. Milani, S. Gladiali, C. Carfagna, B. Binotti, S. Bronco and T. Gragnoli, *J. Organomet. Chem.*, 2005, **690**, 2106-2120.
32.   Z. Saki, I. D'Auria, A. Dall'Anese, B. Milani and C. Pellecchia, *Macromolecules*, 2020, **53**, 9294-9305.
33.   A. Dall'Anese, V. Rosar, L. Cusin, T. Montini, G. Balducci, I. D'Auria, C. Pellecchia, P. Fornasiero, F. Felluga and B. Milani, *Organometallics*, 2019, **38**, 3498-3511.
34.   P. Wucher, P. Roesle, L. Falivene, L. Cavallo, L. Caporaso, I. Göttker-Schnetmann and S. Mecking, *Organometallics*, 2012, **31**, 8505-8515.
35.   K. E. Allen, J. Campos, O. Daugulis and M. Brookhart, *ACS Catalysis*, 2015, **5**, 456-464.
36.   Y. Zhang and Z. Jian, *Macromolecules*, 2020, **53**, 8858-8866.
37.   Q. H. Tran, M. Brookhart and O. Daugulis, *J. Am. Chem. Soc.*, 2020, **142**, 7198-7206.
38.   R. Nakano, L. W. Chung, Y. Watanabe, Y. Okuno, Y. Okumura, S. Ito, K. Morokuma and K. Nozaki, *ACS Catalysis*, 2016, **6**, 6101-6113.
39.   T. Wang, X.-Q. Hao, J.-J. Huang, K. Wang, J.-F. Gong and M.-P. Song, *Organometallics*, 2014, **33**, 194-205.
40.   F. Juliá and P. González-Herrero, *Journal of the American Chemical Society*, 2016, **138**, 5276-5282.
41.   D. J. Tempel, L. K. Johnson, R. L. Huff, P. S. White and M. Brookhart, *J. Am. Chem. Soc.*, 2000, **122**, 6686-6700.

42. A. Zucca, M. A. Cinellu, M. V. Pinna, S. Stoccoro, G. Minghetti, M. Manassero and M. Sansoni, *Organometallics*, 2000, **19**, 4295-4304.

43. A. D'Amora, L. Fanfoni, D. Cozzula, N. Guidolin, E. Zangrando, F. Felluga, S. Gladiali, F. Benedetti and B. Milani, *Organometallics*, 2010, **29**, 4472-4485.

44. S. Stoccoro, B. Soro, G. Minghetti, A. Zucca and M. A. Cinellu, *J. Organomet. Chem.*, 2003, **679**, 1-9.

45. A. Tognon, V. Rosar, N. Demitri, T. Montini, F. Felluga and B. Milani, *Inorg. Chim. Acta*, 2015, **431**, 206-218.

For Table of Contents only
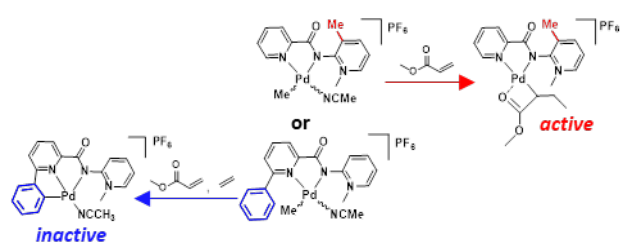
Careful ligand design led to the detection of either an unprecedent, stable, 4-membered palladacycle or an off-cycle catalyst degradation product.